Resource-Efficient Technologies 1 (2018) 36–46

TOMSK POLYTECHNIC UNIVERSITY

Resource-Efficient Technologies

journal homepage: http://ojs.tpu.ru/index.php/res-eff

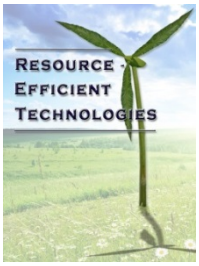


Review article

# ANALYSIS OF A TWO-CRYSTAL DELAY LINE FOR FEMTOSECOND PULSES OF THE X-RAY FREE ELECTRON LASER

**V.A. Bushuev[1],**
vabushuev@yandex.ru

**I.A. Petrov[1],**
ia.petrov@physics.msu.ru

[1] M.V. Lomonosov Moscow State University,
Leninskie Gory, Moscow 119991, Russia.

## Abstract

Using the methods of statistical optics the formation of delayed X-ray pulses in the diffraction reflection of an incident pulse with an arbitrary degree of temporal coherence from a system of parallel crystals with different lattice periods is considered. The results are of interest for constructing delay lines in experiments with a time resolution of the pump-and-probe type and realizing of the self-seeding mode to increase the degree of temporal coherence of the X-ray free-electron laser radiation.
A rigorous theory of dynamic diffraction in Bragg geometry is applied to the diffraction reflection of short X-ray pulses from a system of two parallel crystals with arbitrary thicknesses, and also, for a system of two pairs of parallel crystals. The dependence of the delay time and the intensity of the delayed pulses on the thickness of the crystals and the distances between them are analyzed. Since the pulses from the X-ray free electron laser have high spatial coherence, i. e. a small angular divergence, but very poor temporal coherence, special attention is paid to the effect of the degree of temporal coherence on the width of the energy spectrum of the incident pulses and on the influence of this width on the intensity of the delayed pulses.

*Keywords*: dynamic diffraction theory, short X-ray pulses, delay line, temporal coherence.

## 1. Introduction

For X-ray studies of fast processes in atomic physics, condensed matter physics, physics of high molecular compounds, etc., it is necessary to carry out experiments in the "pump and probe" mode in which one pulse is exciting pulse and the second pulse that incident on the object under investigation with some time delay, is a probing pulse. Lines of delay are also necessary for implementing the self-seeding mode, in order to increase the temporal coherence and monochromaticity of X-ray Free Electron Laser (XFEL) radiation.

With recent launch of European X-ray Free Electron Laser and construction of other free-electron lasers, there's a growing need for effective delay lines which can provide a series of coherent stable femtosecond hard X-ray pulses. At the moment for time-resolved studies with XFEL pulses generated in undulator are going to be sent on samples which will take snapshots of the changes in atomic structure of the sample [1].

☆ Peer review under responsibility of Tomsk Polytechnic University.
https://doi.org/10.18799/24056537/2018/1/181

These 10–100-fs pulses have a highly non-coherent temporal structure and travel with time difference of 200 ns arranged into bunch trains of 3000 pulses arriving with a repetition rate of 10 Hz [2]. The latter limits the temporal resolution at which processes at sub-atomic level can be studied.

To control the delay time, delay lines were proposed in [3–6] consisting of a sufficiently large number (from 3 [6] to 8 [3–5]) of separately located crystals in the reflection and transmission geometries, which imposes stringent conditions on the constant wave-length of radiation, Bragg angles (45° in [3–5], ≈90° in [6]) and the stability of the crystal position. In addition, in [3–6] there are no calculations of the shape and intensity of delayed pulses.

Earlier, in our works [7–9], a dynamical theory of the diffraction of coherent [7] and random [8, 9] X-ray pulses in crystals and multilayer structures was constructed. In [10] we showed that, due to the large spectral width of the incident pulse of the XFEL, its reflection from the multilayer crystal structure and systems of separated parallel crystals leads to the formation of a series of delayed reflected pulses.

In the present paper we consider a more general case, namely, diffraction reflection of pulses with an arbitrary degree of temporal coherence from a plane-layered crystal structure and, in the simplest case, from a bicrystal. Bicrystal is a crystalline film with a thickness $l$ and interplanar distances $d+\Delta d$ lying on a substrate with interplanar distances equal to $d$. The need for such an analysis is due to the fact that XFEL pulses have very mediocre temporal coherence which is characterized by the ratio $\Delta\Omega\tau_0 \sim 10^2$–$10^3$ where $\Delta\Omega$ is the width of the XFEL pulse spectrum, $\tau_0$ is the pulse duration. It is shown how the duration of the incident pulse, the time of its coherence, the thickness and atomic periods of the crystal layers affect the intervals between the delayed pulses, their temporal structure and the relative intensities of the delayed pulses.

The results of this study may be of interest in constructing delay lines for carrying out experiments with a time resolution of the pump-and-probe type and realizing the self-seeding regime.

In this paper two methods for generation of delayed pulses are studied. The first one is diffraction in crystal multilayer structure (MS). Reflection from each layer results in a separate delayed pulses (Fig.1). For the second way we propose a simple and effective delay line design, which consists of two plane-parallel single crystals separated by some air gap $L$ (Fig. 2).

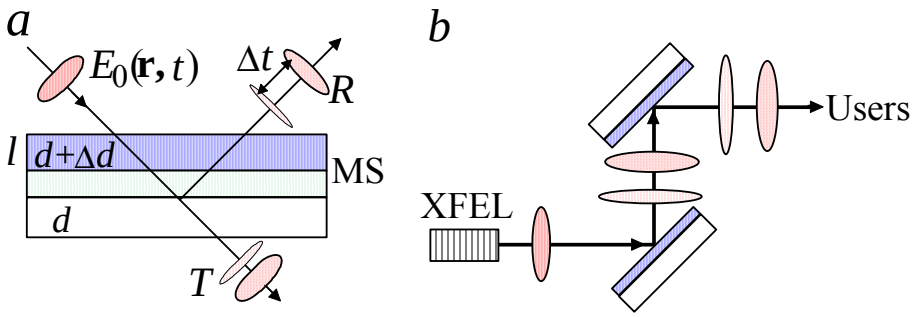


**Fig. 1.** *a* – formation of delayed pulses in crystal multilayer structure;
*b* – orientation of crystals required to maintain the same direction of pulse propagation after all reflections

At experiment it is important to keep the direction in which the pulses travel after reflection. Fig. 1*b* shows that if the pulse is reflected from two same parallel multilayer crystals the direction remains the same and the second reflection results in an additional delayed pulse. It is clear that reflection from a crystal with a bigger number of layers will result in more delayed pulses. Also, variation of thickness allows for different delays.

Another design of the delay line is presented in Fig. 2. Here, an incident pulse is reflected from two distant parallel crystals. The key feature of this design is that various distance between crystals $L$ results in a different delay time. Also, if one takes thin crystals, it is possible to acquire delayed transmitted pulses.

The crystal thicknesses range from fractions to tens of the extinction depths, i. e. $l_{1,2} \propto 5-100\,\mu\text{m}$. Crystals with a larger thickness are not advisable, since this will lead to an increase in the thermal load on the crystal under the action of high-power XFEL pulses. Their interplanar distances differ by a certain small

value $\Delta d$ such that the distance between the peaks of the spectral Bragg reflection is several times greater than the diffraction widths of these peaks. Since the pulses of XFEL are characterized by very comparatively low temporal coherence, the energy spectrum of the incident pulse overlaps both diffraction peaks. As a result, each crystal is reflective in its spectral region in the vicinity of Bragg wavelengths $\lambda_1 = 2d\sin\theta$, and $\lambda_2 = 2(d+\Delta d)\sin\theta$, where $\theta$ is an angle of incidence of the pulse with respect to the crystal surface, and is practically transparent in other spectral regions (Fig. 2). The delay time $\Delta t = 2(l_2 + L)\sin\theta_B / c$ can be smoothly controlled by simply changing the width of the air gap $L$, where $\theta_B$ is the Bragg angle for the crystal 1 and for radiation with a wavelength $\lambda_1$.

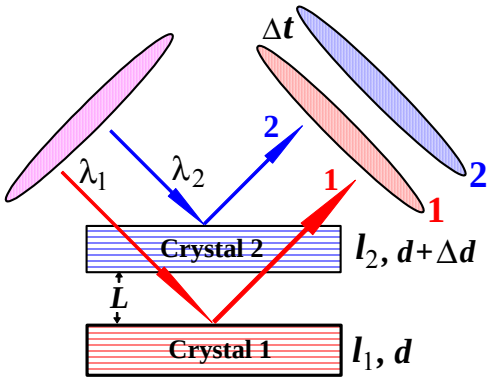


**Fig. 2.** Schematic operation of delay line based on two distant crystals

## 2. Theory

Consider the incidence of a spatially limited pulse with an electric field $E_0(\mathbf{r},t)$ on the crystal or any multilayer or multicrystal system. We will take into account that the XFEL pulses are characterized by a high degree of spatial coherence (~0.71–0.95 [11]) and a very small angular divergence of $\Delta\theta_p \approx 0.2$–$0.4$ arc.sec [11]. This divergence is much less than the angular width of Bragg reflections of $\Delta\theta_B$ ~1–3 arc.sec (for reflections (400), (220) and (111) from diamond crystals of radiation with a wavelength of $\lambda = 0.1$ nm [12]). Therefore, one can use the wave packet model with an electric field $E_0(t) = A_0(t)\exp(-i\omega_0 t)$, where $A_0(t)$ is the slowly varying field amplitude and $\omega_0$ is the central frequency.

Statistical optics approach was used to describe the intrinsic random structure of the pulse. According to [2, 11] a ~10–100 fs SASE1 pulse consists of a set of spikes with estimated coherence time of ~0.2 fs. In [8, 9] it is shown that this random field amplitude can be approximated as (Fig. 3):

$$A_0(t) = F_0(t)\,a(t), \tag{1}$$

where $F_0(t)$ is the incident-pulse envelope, $a(t)$ is a random stationary process which average amplitude $< a(t) >= 0$, average intensity (dispersion) $< a(t)a^*(t) >= 1$ and the temporal-coherence function $\gamma(\tau) =< a(t)a^*(t+\tau) >$ are independent of time $t$.

Let us write the random amplitude of a pulse incident on a crystal, $A_0(t)$ in Eq. (1) as an expansion in a Fourier integral:

$$A_0(t) = \int_{-\infty}^{\infty} A_0(\Omega)\exp(-i\Omega t)d\Omega, \tag{2}$$

where $\Omega = \omega - \omega_0$, $\omega_0 = 2\pi c/\lambda$, and the spectral amplitude

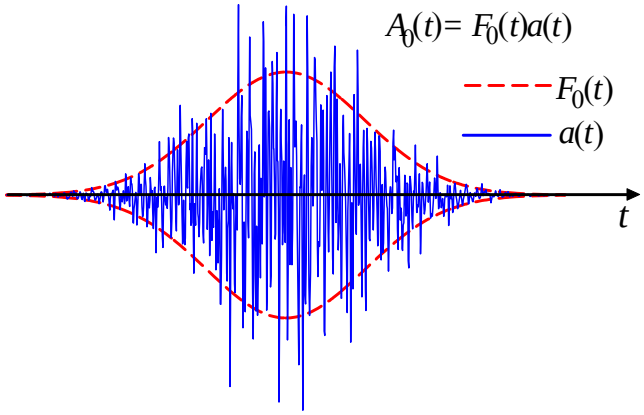


**Fig. 3.** Schematic representation of random XFEL pulse

$$A_0(\Omega) = (1/2\pi) \int_{-\infty}^{\infty} A_0(t) \exp(i\Omega t) d\Omega. \tag{3}$$

Since the pulse amplitude $A_0(t)$ is random, $A_0(\Omega)$ in Eqs. (2) and (3) is also a random function. Since each plane wave with an spectral amplitude $A_0(\Omega)$ which is incident on a crystal and makes an angle $\theta = \theta_B + \Delta\theta$ with the crystal surface, is reflected from the crystal (or systems of crystals) with the complex amplitude coefficient $R(\Omega)$, the reflected pulse amplitude is determined by the integral [7]:

$$A_R(t) = \int_{-\infty}^{+\infty} A_0(\Omega) R(\Omega) \exp(-i\Omega t) d\Omega. \tag{4}$$

Furthermore, we will assume for definiteness that the incident-pulse envelope $F_0(t)$ in Eq. (1) and the temporal-coherence function $\gamma(\tau)$ of a random process $a(t)$ are Gaussians: $F_0(t) = \exp(-t^2/\tau_0^2)$, where $\tau_0$ is pulse duration, and $\gamma(\tau) = \exp(-\tau^2/\tau_c^2)$, where $\tau_c$ is the coherence time. The envelop spectrum amplitude $F_0(\Omega)$ and the spectral density $G(\Omega)$ of random signal $a(t)$ are

$$F_0(\Omega) = \frac{\tau_0}{2\sqrt{\pi}} \exp\left(-\Omega^2 \tau_0^2/4\right), \quad G(\Omega) = \frac{\tau_c}{2\sqrt{\pi}} \exp\left(-\Omega^2 \tau_c^2/4\right), \tag{5}$$

where spectral density according to the Wiener–Khinchin theorem is

$$G(\Omega) = (1/2\pi) \int_{-\infty}^{\infty} \gamma(\tau) \exp(-i\Omega\tau) d\tau. \tag{6}$$

For expression (1), one cannot use Eq. (4) in simple analytical form for calculation of reflected intensity $I_R(t) = |A_R(t)|^2$ as the signal cannot be calculated due to its random structure. However, intensity of the pulse can be derived with the use of statistical optics [9]:

$$I_R(t) = \left\langle |A_R(t)|^2 \right\rangle = \int_{-\infty}^{\infty} \int_{-\infty}^{\infty} \left\langle A_0(\Omega) A_0^*(\Omega') \right\rangle R(\Omega) R^*(\Omega') \exp\left[-i(\Omega - \Omega')t\right] d\Omega d\Omega', \tag{7}$$

where

$$\left\langle A_0(\Omega) A_0(\Omega')\right\rangle = \frac{\tau_0\tau_c}{4\pi\sqrt{2(1+\xi)}} \exp\left[-\frac{(\Omega-\Omega')^2\tau_0^2}{8(1+\xi)} - \frac{\left(\Omega^2+\Omega'^2\right)\tau_c^2}{8(1+\xi)}\right] \quad (8)$$

is the spectral correlation function [9], $\xi = \tau_c^2 \Big/ \left(2\tau_0^2\right)$.

## 3. Results and discussion

One of the ways to generate coherent delayed pulses is reflection in multilayer crystals (Fig. 1). During growth of diamond crystals, addition of boron dopant atoms increases interplanar spacing in a layer, which leads to the difference of Bragg angles for thin layers grown on thick crystals. In [13], it was demonstrated that such method results in separate Bragg peaks after doping of diamond crystal. For definiteness we consider the case of X-ray radiation with the wavelength $\lambda = 0.1$ nm for all presented results. The wavelength is chosen to be close to photons energy 12.4 KeV – first-harmonic signal of SASE1 channel at European XFEL [2].

Fig. 4 shows spectral reflection curves for a semi-infinite crystal with a 10 μm doped layer for two different interplanar spacing $\Delta d$ in the layer. It is clear that a larger interplanar spacing difference yields larger Bragg angle and, accordingly, Bragg spectral frequency difference for layer and substrate. This means that different spectral components reflect from different layers and gives two delayed pulses. Fig. 5 shows temporal structure of a pulse reflected from a double-layer crystal (bicrystal).

Reflected pulses have roughly the same intensity because spectral density of random signal $G(\Omega)$ is much wider than wave-packet spectrum $F_0(\Omega)$. That way each peak intensity is defined by the area under each reflection peak, which is similar for both peaks, even though their peak values are different. As can be seen from Fig. 5, for thicker layers dynamical effects are more significant, and it results in a more complex temporal structure.

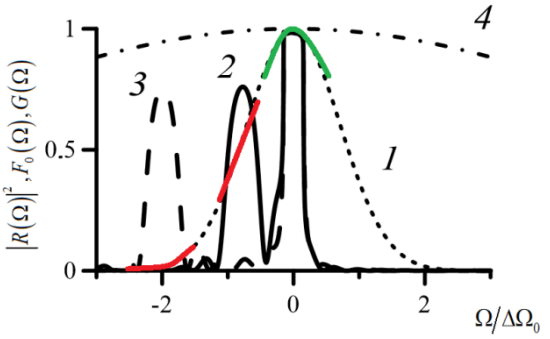


**Fig. 4.** 1 – incident wave-packet spectrum $F_0$ of envelop with width, $\Delta\Omega_0 = 2/\tau_0$; 2, 3 – reflection curves for $\Delta d/d = 2\cdot10^{-5}$ and $\Delta d/d = 5\cdot10^{-5}$, respectively, $d$ is interplanar spacing for undoped C(400), $\Delta d$ is interplanar spacing difference for the layer and substrate

Here $\tau_0 = 5$ fs is duration of the pulse, i. e. the width of the wave-packet, thickness of the layer is $l = 10$ μm, green and red curves represent different spectral components that will form separate delayed pulses, *4* – spectral density of random signal $G(\Omega)$, coherence time $\tau_c = 0.2$ fs

Growth techniques of multilayer crystals are still to be developed, as the interface smoothness is crucial for the presented design, as well as absence of structural defects which are likely to be caused by dopants. One should keep it in mind that delay pulses reflected at the same angles only in the case of symmetrical Bragg reflection (see also [7]).

Above we considered the delay lines for XFEL pulses with a low degree of coherence, for which the condition $\Delta\Omega >> \Delta\Omega_B$ is satisfied, where $\Delta\Omega_B = \omega_0|\chi_h|/\sin^2\theta_B$ is the spectral width of the Bragg

reflection, and $\chi_h$ is the Fourier component of the crystal polarizability. It is also of interest to consider the possibility of creating a delay line for high-coherence pulses obtained using the self-seeding scheme and for which the coherence time is $\tau_c \le \tau_0$.

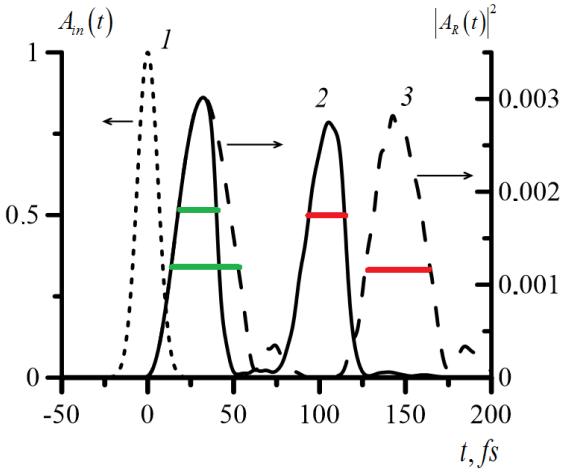


**Fig. 5.** 1 – wave-packet of an incident $\tau_0 = 5$ fs pulse with $\tau_c = 0.2$ fs coherence time; 2, 3 – temporal structure of the pulse after reflection from a double-layer crystal with layers' thicknesses $l_1 = l_2 = 10$ μm and $l_1 = l_2 = 15$ μm, deformation is $\Delta d/d = 2 \cdot 10^{-5}$ for both layers, C(400). Colored waists of the pulses depict delayed pulses generated by different spectral components of the pulse for different thickness of the layer (Fig. 4, peaks *1* and *2*)

In this case, the spectrum of the incident pulses sharply narrows. Therefore the bicrystal must be rotated at such an angle $\Delta\theta$ with respect to the Bragg angle $\theta_B$, so that the maximum of the pulse spectrum lies approximately in the middle between the reflection peaks from the film and from the substrate (Fig. 6). In this case, the delayed pulses are formed as a result of the diffraction of radiation concentrated on the "tails" of the incident pulse spectrum, which fall in the region of the Bragg reflection peaks from the film and from the substrate. This situation is presented in Fig. 6. It can be seen, as in Fig. 5, as with the increase in the thickness of the film, the delayed pulse shifts to the region of larger times.

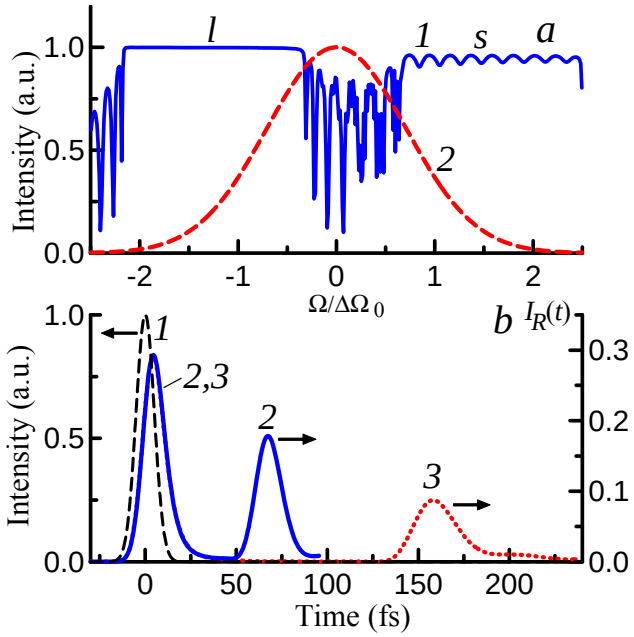


**Fig. 6.** Panel *a*: 1 – spectral reflection curve with reflection peaks from the layer (*l*) and from the substrate (*s*); 2 – incident pulse spectrum; parameters: $\tau_0 = 10$ fs, $\Delta d/d = 3 \cdot 10^{-5}$, $\Delta\theta = -1.5$ arc. sec, $l = 50$ μm, C(400). Panel *b*: 1 – incident pulse, curves 2 and 3 – delayed pulses at layer thicknesses $l = 20$ μm (*2*) and $l = 50$ μm (*3*)

It is easy to see that the delay time in the case of diffraction reflection of a pulse from a bicrystal, as it is shown in Fig. 1 and Fig. 3–6, is determined mainly by the thickness of the upper layer: $\Delta t \approx 2l \sin\theta_B / c$. From a practical point of view, this is not very convenient, since for a smooth adjustment of the delay time, a large set of bicrystals with different thicknesses $l$ is required.

However, the situation is greatly simplified if instead of bicrystal we use a system of two parallel crystals separated by a certain interval $L$, the value of which can be smoothly changed (Fig. 2). Moreover, instead of such a very complicated procedure as ion implantation, one can use simple heating of one of the crystals to change the interplanar distances in crystals. In this case, the relative change (deformation) is equal of $\Delta d / d = \alpha_T \Delta T$, where $\alpha_T$ is the coefficient of linear thermal expansion, and $\Delta T$ is the change of a temperature. At a temperature of 300 K, the coefficient of thermal expansion of crystal of synthetic diamond is $\alpha_T = 1 \cdot 10^{-6}$ [14]. Hence it follows that to ensure, for example, the magnitude of the crystal deformation $\Delta d / d = 2 \cdot 10^{-5}$, as in Fig. 5, one of the two crystals needs to be heated only by $\Delta T = 20^0$C.

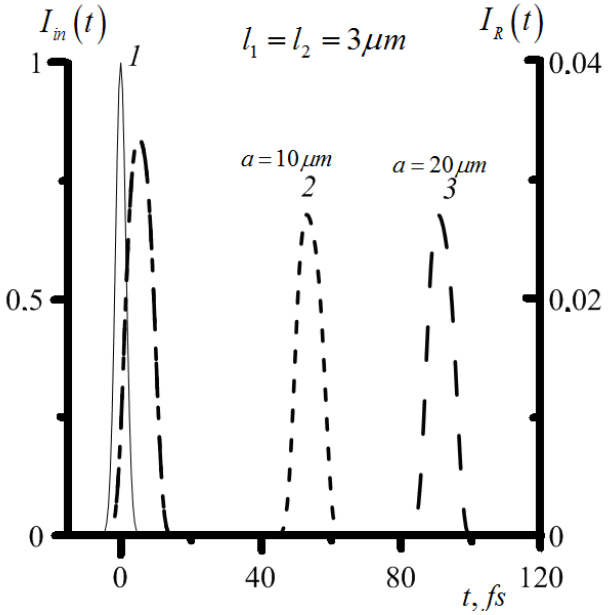


**Fig. 7.** *1* – incident pulse, *2, 3* – reflected pulses temporal structure for $a = L = 10$ μm and $a = L = 20$ μm, respectively. Crystals have the same thickness of $l_1 = l_2 = 3$ μm, diamond (400). Reflected pulse intensity is presented on the right-side axis

Fig. 7 shows that different distance between crystals leads to different delays. However, at the moment it appears to be impossible to grow crystals as thin as 3 μm, so generation of desired smooth separate peaks is not feasible.

Fig. 8 shows the delayed pulse curves for different values of the width of the gap $L$ between the crystals. It can be seen that the delay time $\Delta t$ increases linearly with increasing of the distance $L$. The pulses intensities do not depend on this distance. It follows from Fig. 8 that there is some "dead" time delay $\Delta t \approx 130$fs under the width of the gap $L = 0$. This time is determined by the thickness of the upper crystal 2 (with deformation) in Fig. 2. To reduce the delay time, this thickness should be reduced. However, in this case the intensity of the delayed pulse also decrease and the pulse shape change.

This problem can be solved in a simpler way. For this it is necessary in the second system of crystals to interchange the crystals with deformation and without deformation. In this case, the "fast" pulse reflected from the upper crystal with deformation in the first system of crystals at first falls on the ideal crystal in the second system of crystals, passes through it and is reflected from the crystal with deformation. The delay time of this pulse increases as a result of passing through an ideal first crystal. On the other hand, the delayed pulse which is formed by reflection from the lower ideal crystal in the first system of crystals is immediately reflected practically without delay from the ideal crystal in the second system. Thus, the delay time can be reduced almost to zero.

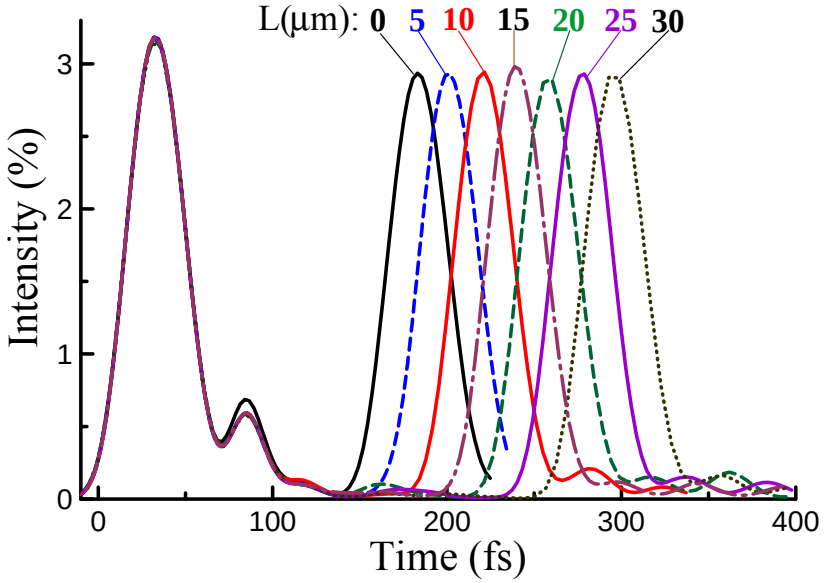


**Fig. 8.** Demonstration of the time structure of delayed pulses depending on the thickness $L$ of the gap between the crystals. Parameters: $l_1 = 20\mu m$, $l_2 = 50\mu m$, $\Delta d/d = 3\times10^{-5}$, duration of the incident pulse $\tau_0 = 20fs$, coherence time $\tau_c = 2fs$

To create an effective delay line, it is very important to be able to control the intensities of delayed pulses. Let us consider this question in more details. As was shown in Section 2, the amplitude of the reflected pulse is determined by the following integral relation

$$A_R(t) = \int_{-\infty}^{+\infty} A_0(\Omega) R(\Omega) \exp(-i\Omega t)\, d\Omega$$

where under the integral sign is the product $A_0(\Omega)R(\Omega)$ of the amplitude of the incident pulse spectrum $A_0(\Omega)$ on the spectral amplitude of the reflection coefficient $R(\Omega)$ of our crystal structure. Therefore, to change the amplitude $A_R(t)$ of the reflected pulse, one can use the fact that the reflection coefficient $R(\Omega)$ depends on the crystal thickness, on the degree of deformation, on the reflection order, and the pulse spectrum $A_0(\Omega)$ depends on the pulse duration and the coherence time. In addition, the position of the spectrum relative to the diffraction reflection curve depends on the angular deviation of the crystals with respect to the Bragg angle.

Below we consider two possibilities for controlling the intensity of delayed pulses. Fig. 9 shows how the relative arrangement of the diffraction reflection curves with respect to the spectrum of the incident pulse changes with a change of the degree of deformation $\Delta d/d$. It is clear that the product of the curve of the spectrum *4* by the diffraction reflection curve *1*, which corresponds to the value of the crystal deformation $\Delta d/d = 3\times10^{-5}$, is several times larger than the product of the weak "tail" of the spectrum (curve *4*) by curve *3* which corresponds to an increased degree of deformation $\Delta d/d = 9\times10^{-5}$.

The second possibility of controlling the amplitude of the reflected pulses is due to the fact that the amplitude reflection coefficient depends on the crystal thickness, and specifically its magnitude increases with increasing crystal thickness. Fig. 10 shows the spectral reflection curves for a fixed degree of deformation $\Delta d/d = 4\times10^{-5}$, but for three different thicknesses $l_2$ of the second crystal. It is clear that the above product $A_0(\Omega)R(\Omega)$ in the region of the spectrum corresponding to the reflection from the second crystal will increase with increasing thickness $l_2$ while the same product does not depend on this thickness in the central region of the reflection spectrum $\Omega \approx 0$ from the undeformed first crystal.

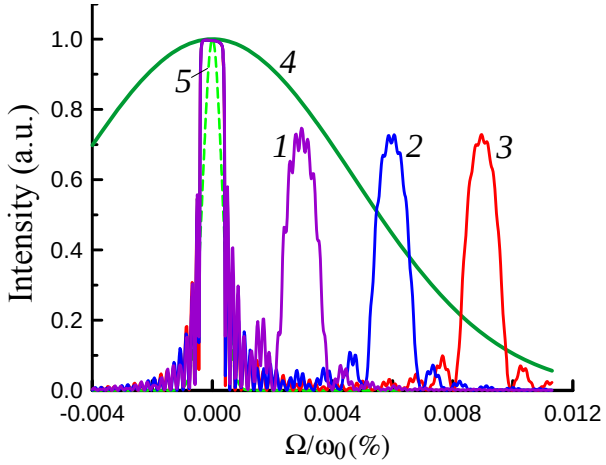


**Fig. 9.** Spectral curves of diffraction reflection 1–3 depending on the degree of deformation $\Delta d/d$, 4 – spectrum of the incident pulse, 5 – spectrum of the pulse envelope; curve 1 – $\Delta d/d = 3\times10^{-5}$, angle deviation $\Delta\theta = -4.2$arc.sec; curve 2 – $\Delta d/d = 6\times10^{-5}$, $\Delta\theta = -8.4$arc.sec; curve 3 – $\Delta d/d = 9\times10^{-5}$, $\Delta\theta = -12.6$arc.sec. Parameters: $l_1 = 40$μm, $l_2 = 10$μm, $\tau_0 = 20$fs, $\tau_c = 2$fs, synthetic diamond crystals, reflections (400)

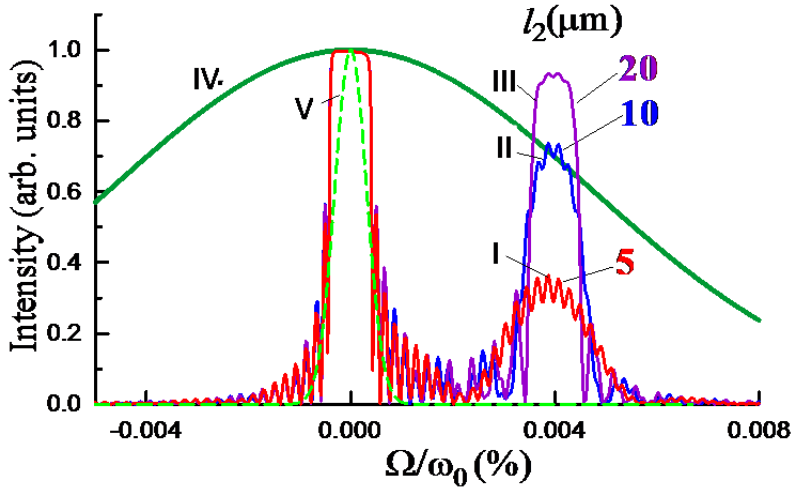


**Fig. 10.** The spectral reflection coefficient (curves I–III) for different thicknesses of the second crystal (the thicknesses are indicated in the figure), the spectrum of the incident pulse (curve IV) and the spectrum of its envelope (curve V). Parameters: deformation of the second crystal diamond crystals, reflections (400)

In Fig. 11 reflected pulse temporal structure is shown for three 20 μm-thick crystals. Here, stronger dynamical effects compared to the case with thin crystals take place resulting in irregular temporal structure and secondary peaks.

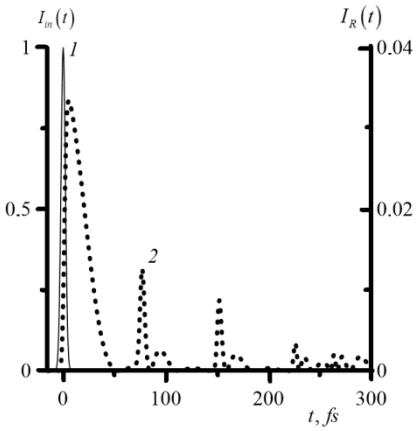


**Fig. 11**. 1 – incident pulse (left axis), 2 – reflected pulse (right axis) in case of three 20 μm-thick crystals positioned at a distance of $L = 10$ μm from each other

The presented designs have a potential to generate delayed XFEL pulses at sub-100 fs level with regular temporal structure. Also small number of optical elements required makes the introduced delay line easy to operate. Unlike previously introduced delay lines [3–6], diffraction in only two crystals produces delayed pulses. Moreover, the presented delay line allows for operation at any energy by simultaneous rotation of the crystals, adjusting incidence angle to an arbitrary central energy of the incident pulse.

## 4. Conclusion

Thus, in this paper we analyze a simple X-ray delay line which consists of one and (or) two blocks. Each block represents two fairly perfect crystals with thicknesses $l_1$ and $l_2$ and parallel to each other. The interplanar distances in one of the crystals (for example, in the first crystal with thickness $l_1$) differ by some amount $\Delta d$ from the other crystal. The distances between the crystals in the 1st and 2nd blocks are equal to $L_1$ and $L_2$, respectively. The delay time for diffraction at the first block is approximately equal to $\Delta t_1 = 2(l_1 + L_1)\sin\theta_B / c$. The minimum delay time is realized when $L_1 = 0$. In other words, there is a so-called "dead time" delay, the magnitude of which $\Delta t_1 = 2l_1 \sin\theta_B / c$ is determined by the thickness $l_1$ and cannot be made very small since the intensity of the diffraction reflection simultaneously decreases sharply.

The second block is necessary in order to preserve the direction of propagation of the delayed pulses with respect to the incident pulses. If in the second block the first crystal is also a crystal with a thickness $l_1$, then the delay time is equal to $\Delta t = 2\Delta t_1$, i. e. it increases. However, if the first crystal is the crystal with $\Delta d = 0$ and whose thickness is $l_2$, then the delay time becomes equal to the difference $\Delta t = 2[(l_1 + L_1) - (l_2 + L_2)]\sin\theta_B / c$. It is easy to see that a simple change in the distances between the crystals leads to the fact that the delay time can be positive, equal to zero (delayed pulses coincide) and even negative (delayed pulses are interchanged).

Unlike previous schemes [3–6], this delay line can operate in a wide range of wavelengths which is achieved by a simple rotation of all the crystals. In addition, calculations of the intensities of delayed pulses in relation to the duration of the incident pulses, the coherence time, and the crystal thicknesses were performed in this paper.

It is quite clear that in real situations there will be a number of problems associated with ensuring the parallelism of the crystals, specifying the required deformation and also the quite possible non-stationary heating of all crystals under the action of a powerful thermal load due to the partial absorption of the energy of the incident pulses. These and similar questions require further investigation.

## Acknowledgments

This work was supported by the Russian Foundation for Basic Research, project No. 16-02-00887.

## Conflict of interest

The authors declare no conflict of interest.

## References

[1] Altarelli M. et al., XFEL: The European X-ray Free-electron Laser. *Technical Design Report. DESY*, 2006, vol. 6, no. 97, p. 630.

[2] The European Laser Project XFEL. URL: http://xfel.desy.de/.

[3] Joksch S., Graeff W., Hastings J., Siddins D.P. Performance of an x-ray optical time delay line with synchrotron radiation. *Review of Scientific Instruments*, 1992, vol. 63, no.1, pp.1114–1118. DOI: 10.1063/1.1143110.

[4] Roseker W., Franz H., Ehnes A. et al. Performance of a picosecond x-ray delay line unit at 8.39 keV. *Optics Letters*, 2009, vol. 34, no. 12, pp. 1768–1770. DOI: 10.1364/OL.34.001768.

[5] Roseker W., Franz H., Schulte-Schrepping H., *et al*., Development of a hard X-ray delay line for X-ray photon correlation spectroscopy and jitter-free pump-probe experiments at X-ray free-electron laser sources. *Journal of Synchrotron Radiation,* 2011, vol. 18, no. 4, pp. 481–491. DOI: https://doi.org/10.1107/S0909049511004511.

[6] Stetsko Y.P., Shvyd'ko Y.V., Stephenson G.B. Time-delayed beam splitting with energy separation of x-ray channels. *Applied Physics Letters*, 2013, vol. 103, no. 17, pp. 1–5. DOI: 10.1063/1.4826251, https://aip.scitation.org/doi/pdf/10.1063/1.4826251.

[7] Bushuev V.A. Diffraction of X-ray free-electron laser femtosecond pulses on single crystals in the Bragg and Laue geometry. *Journal of Synchrotron Radiation,* 2008, vol. 15, no. 4, pp. 495–505. DOI: 10.1107/S0909049508019602.

[8] Bushuev V.A., Samoylova L. Application of quasi-forbidden multilayer Bragg reflection for monochromatization of hard X-ray FEL SASE pulses. *Nuclear Instruments and Methods in Physics Research Section A: Accelerators, Spectrometers, Detectors and Associated Equipment*, 2011, vol. 635, no. 4, pp. s19–s23. DOI: 10.1016/j.nima.2010.10.036.

[9] Bushuev V.A., Samoylova L. Influence of Diffraction in Crystals on the Coherence Properties of X-Ray Free-Electron Laser Pulses. *Crystallography Reports*, 2011, vol. 56, no. 5, pp. 819–827. DOI: 10.1134/S1063774511050063.

[10] Bushuev V., Samoylova L., Sinn H., Tschentscher T. Temporal and coherence properties of hard X-ray FEL radiation following Bragg diffraction by crystals. *Proc. SPIE*, 2011, vol. 8141, p. 14. DOI: 10.1117/12.893054.

[11] Tschentscher Th 2011 Layout of the X-Ray Systems at the European XFEL (Technical Report). URL: https://www.xfel.eu/sites/sites_custom/site_xfel/content/e35165/e46561/e46889/e46891/xfel_file46892/TR-2011-003_CDR_WP85_eng.pdf.

[12] X-ray server. URL: http://sergey.gmca.aps.anl.gov/.

[13] Brunet F. et al. The effect of boron doping on the lattice parameter of homoepitaxial diamond films. *Diamond and Related Materials,*1998*,* vol. **7**, no. 6, pp. 869–873. DOI: 10.1016/S0925-9635(97)00316-6.

[14] Obukhov, A.I. and Grigor'ev, I.S. Fizicheskie velichiny: Spravochnik (Physical Quantities: Handbook). Moscow: Energoatomizdat, 1991, p. 1094. in Rus.